Partial Discharge Localization in Transformers Using UHF Detection Method

H. H. Sinaga
The University of New South Wales, Sydney 2052, Australia
and Lampung University, Indonesia

B. T. Phung and **T. R. Blackburn**
The University of New South Wales, Sydney 2052, Australia

ABSTRACT

The location of a partial discharge (PD) source inside a transformer can be determined from the time differences of arrival (TDOA) between signals that are captured by an array of UHF sensors. The TDOA can be acquired from the received PD waveforms. In this paper, three different methods of acquiring the TDOA from the PD waveforms are discussed. The time difference can be calculated either by taking the first peak of the signal as the arrival instant, or from the cross-correlation of the PD waveforms, or by applying the similarity function to the plots of the PD signals cumulative energy. Computation algorithms for determining the TDOA automatically are introduced so that possible bias from human interpretation is avoided. The presence of noise and its effect on the accuracy of the PD localization will also be presented. Experimental results show the first-peak method has higher accuracy than the two other methods. The application of signal denoising further improves the localization accuracy.

Index Terms — **Partial discharge location, transformer diagnostics, UHF measurement.**

1 INTRODUCTION

THE ultra high frequency (UHF) detection of partial discharges (PD) involves the use of UHF sensors (antennas) to capture the fast electromagnetic transients emitted from the discharge site. This detection method has proven viable in monitoring the insulation condition of GIS. It is now being extended and applied to transformer diagnostics [1, 2]. In order to determine the PD location, a distributed array of three or more sensors is used to record the PD signals simultaneously and enable triangulation. The received signals can be processed to determine the arrival time difference between them. Localization of the PD source then can be determined from the time difference of arrival (TDOA) between the sensors.

The detected PD pulse signals are often very weak even for well-designed UHF antennas with high sensitivity. The situation is further exacerbated by the interference from unwanted signals or noise, although it should be noted that the transformer metal tank and graded bushings can provide good shielding against radiative interference. Typical interferences in the UHF range consist of digital radio, television and telecommunication signals, thermal noise in the detection system and periodic pulses from switching operations [3-5]. This can affect the accuracy of the time difference measurement and lead to a false location result. If needed, the PD signals can be denoised to remove the unwanted interference and noise before further analysis is carried out. One of available techniques to denoise multiple signals is the multivariate denoising method. This technique is an improvement of the direct univariate denoising, achieved through the use of principal component analysis (PCA). It has been shown to perform well when applied to denoise signals obtained from multi-channel recording [6].

The determination of the TDOA values from the PD waveforms recorded can be done in several ways. In one approach, the time of arrival (TOA) of the signal is determined by searching for the first peak, i.e. the earliest instant when the magnitude of the received signal reaches a peak value [7-10]. Then the TDOAs between different sensor signals can be computed from the TOAs. Although this method shows high accuracy, the TOAs are determined by visually examining the signals. Thus it is susceptible to the observer's interpretation and possible errors. In another method, the TDOA is found from the cross-correlation between PD signals [9]. The idea is based on the assumption that there is a correlation between signals captured by different sensors because these signals were emitted by the same PD source. However, it was noted that sensors at different positions tend to show different waveform patterns

Manuscript received on 16 January 2012, final version on 16 April 2012.

[10]. The third method examines the cumulative energy of the signals [7, 9-11]. From the energy curve, the time difference between signals is determined by finding the 'knee point' where the change in the signal amplitude is 'sudden'. Although this was achieved based on human judgment to locate the knee point manually [7], automated procedures employed in dielectric dissipation factor (tanδ) measurements can potentially be used for this task.

In this paper the three above-mentioned methods are investigated to locate the PD source and their performance compared. The TDOA values are calculated solely based on mathematic formulas thus removing possible ambiguity from human interference. A specific threshold value enables an algorithm to determine the first peak. The TDOA can also be derived from where the cross-correlation between two signals reaches its maximum value. Alternatively, a similarity function between two cumulative energy curves is evaluated to search for the minimum.

As aforementioned, it is important to denoise the waveform to reveal the original signals. Although the denoising process may be able to reduce or eliminate noise from the original signals, it may also alter the signals and thus cause error in determining the TDOA values. Furthermore, it increases computational burden significantly [10]. The effect of the denoising process is also discussed in this paper. The PD waveforms are denoised by applying a Matlab multivariate denoising tool and subsequently the PD location is calculated using the acquired TDOA values. The location results from using undenoised and denoised waveforms are compared to demonstrate the benefits of the denoising process.

2 TIME DIFFERENCE OF ARRIVAL

In general, the sensors should be placed far apart so to increase the possibility of getting significant difference between the signal arrival times. This will help reduce measurement uncertainty and thus improve triangulation accuracy. Consider an arbitrary array of PD sensors installed at different locations in a transformer tank. Electromagnetic waves emitted by a PD source propagate in the transformer tank and arrive at these sensors at different time instants. Denote t_1 the time of arrival (TOA) at sensor 1, t_2 the TOA at sensor 2, etc. The time difference of signal arrival (TDOA) between sensor 1 and 2 is then defined as:

$$\Delta t_{12} = t_1 - t_2 \tag{1}$$

Measurement of the time of arrival (TOA) of PD signals is affected by a number of factors. The presence of noise alters the PD waveform. The sensor captures not only the PD signals but also background noise surrounding the sensor. The PD signals often are very weak and have very low amplitude even for well-designed sensors [10].

Another contributing factor is the sensors response time. Different sensors have different responses [12] and resulted in different waveforms [10]. The installed position of sensors can affect the wave shape of the received signals. Sensors at close proximity will give similar responses to the same PD but this is not so for those far apart because of the distortion from the transmission medium.

Measurement of the TOA is also affected by the rise time of the PD current pulse. Different types of insulation faults or defects will generate different PD pulses. For example, a PD of 1 ns pulse width already spreads over a distance of 20cm in term of radiated electromagnetic signals and thus causes uncertainty in that order of magnitude in the location. In some cases, the PD pulse rise time can be considerable, up to 17 ns for bad contacts in oil [13] and hence a higher location error.

3 LOCATING THE PD SOURCE

After PD signals are generated from the origin location, the signals will emanate in all directions at the same propagation velocity, with the assumption that the surrounding environment is homogeneous. The sensors are placed at arbitrary locations with different distances from the PD source and so will receive the signals at different time instants. A closer sensor detects signals before the one further away. Thus there is time delay among the received signals. This time delay is correlated to the distance of the PD source to the sensors.

The distance of the PD source to sensor can be calculated using Pythagorean theorem. For any sensor i of an array as illustrated in Figure 1:

$$r_i^2 = (x - x_i)^2 + (y - y_i)^2 + (z - z_i)^2 \tag{2}$$

where (x, y, z) are the coordinates of the PD source and (x_i, y_i, z_i) are the coordinates of sensor i.

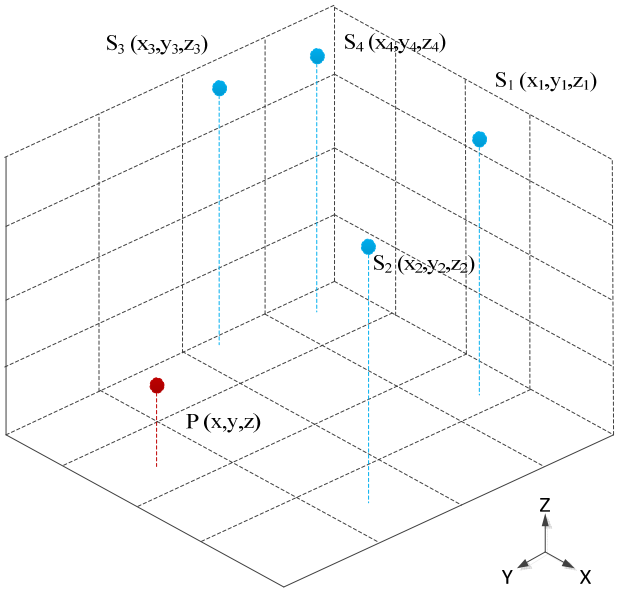

Figure 1. Coordinate system of PD source P (x,y,z) and sensor S_i (x_i, y_i, z_i).

In order to triangulate and determine the PD source, it is necessary to apply at least four sensors to record the PD signals simultaneously. With the sensors position known and measurement of the differences in the times of signal arrival at the sensors, the PD location can be found which corresponds to the intersection of the hyperbolic curves defined by the TDOAs.

A number of computation methods were proposed to determine the signal source by solving the set of non-linear equations in the form of equation (2). The number of equations in the set corresponds to the number of sensors in use. A common method is the Newton-Raphson which applies Taylor series expansion to linearize those equations [14, 15]. In [16], a fuzzy method was used to find the solution. However, the computation is iterative and can be extensive in some cases to achieve convergence. Subsequently, a more elegant method was introduced in [17, 18] whereby the explicit solution for the location is determined from the TDOAs by using an approximate realization of the maximum-likelihood estimator. This method is very efficient (non-iterative) and so it is adopted in this work.

When four sensors are applied to capture PD signals and the sensors are positioned randomly, the coordinate of the PD source can be written in terms of the distance between the PD source and a reference sensor [18]. Without loss of generality, choose (r_4) as the reference sensor, it can be shown that:

$$\begin{bmatrix} x \\ y \\ z \end{bmatrix} = -\begin{bmatrix} x_{14} & y_{14} & z_{14} \\ x_{24} & y_{24} & z_{24} \\ x_{34} & y_{34} & z_{34} \end{bmatrix}^{-1} \times \left\{ \begin{bmatrix} r_{14} \\ r_{24} \\ r_{34} \end{bmatrix} r_4 + \frac{1}{2} \begin{bmatrix} r_{14}^2 - K_1 + K_4 \\ r_{24}^2 - K_2 + K_4 \\ r_{34}^2 - K_3 + K_4 \end{bmatrix} \right\} \quad (3)$$

where (x,y,z) are the coordinates of the PD source, (x_{i4}, y_{i4}, z_{i4}) denote differences in coordinates between sensor 'i' and the reference sensor (sensor 4), r_{i4} is the TDOA between sensor i and sensor 4 times the speed of the PD signal in oil, r_4 is the distance of sensor 4 to the PD source and K_i is calculated as $K_i = x_i^2 + y_i^2 + z_i^2$. Note that all the parameters on the right-hand side of equation (3) are known except r_4. Utilizing this equation, one can substitute x,y,z in term of r_4 into equation (2) and solve that quadratic equation. The positive root value of r_4 acquired from equation (2) is then input back into equation (3) to determine the PD source coordinates.

4 EXPERIMENTAL SET-UP

Figure 2 shows the experimental setup which makes use of the steel tank of a small distribution transformer. The tank has dimension of 71.5 cm in width, 118 cm in length, and 95 cm in height. The core and windings were removed from the tank so the existing oil level dropped down to about half-height (50cm). Without these physical obstructions, the artificial PD source can be easily moved to various locations within the oil volume and the sensors have direct line-of-sight to the PD source. The sensors were positioned close to the tank wall to simulate their mounting on the wall. The tank was fully enclosed. High voltage connection to a discharge source placed inside the tank was made via a high-voltage bushing. It must be stressed that the test setup is relatively small and simplified as compared to large power transformers. Complications can arise from effects of solid physical barriers in the tank on the PD signal propagation.

Four UHF sensors were applied to capture the PD signals. Their outputs were connected to a 40 Gs/s four-channel digital oscilloscope via coaxial cables of identical length. The sensors and the PD source were immersed in oil and their coordinates are shown in Table 1. The PD source was a needle-plate electrode arrangement and was moved to 12 different locations. The coordinates of these locations are shown in Table 2. For each PD location, 50 sets of PD waveforms were recorded and used in the analysis. The TDOAs of these waveforms are then used to determine the PD location.

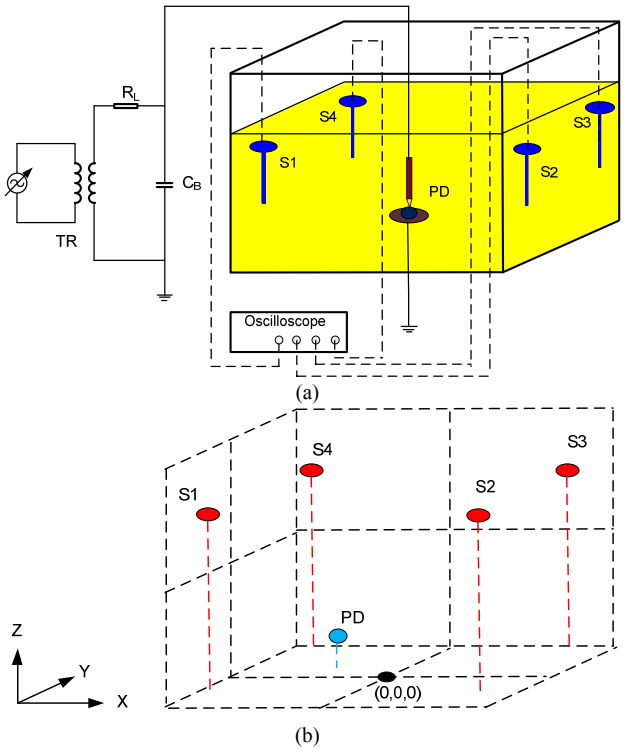

Figure 2. Experimental setup: (a) layout and circuit for PD generation and detection, (b) coordinate system for location.

Table 1. UHF sensors position

	x (cm)	y (cm)	z (cm)
Sensor 1	-50	-25	48
Sensor 2	45	-20	46
Sensor 3	45	20	49
Sensor 4	-50	20	45

Table 2. PD source coordinates

Position No.	x (cm)	y (cm)	z (cm)
1	-11	14	37
2	-11	5	37
3	-11	-4	37
4	-3	14	37
5	-3	5	37
6	-3	-4	37
7	6	15	37
8	6	5	37
9	6	-5	37
10	12	15	37
11	12	5	37
12	12	-5	37

5 PD SIGNALS

5.1 SIGNALS PROPAGATION

To determine the distance of the travelling electromagnetic signals in the transformer, the velocity of the signals has to be known first. In air, the propagation velocity of the

electromagnetic signals is the speed of light, i.e. $3x10^8$ m/s. According to the well-known Maxwell's theory, the propagation velocity of electromagnetic waves in a given medium is $v = 1/\sqrt{\mu\varepsilon}$ where μ is the permeability and ε is the permittivity of the medium. In oil, the propagation velocity would be slower because of its higher permittivity as compared to air, the latter has a relative permittivity of 1. Without exact manufacturer data on the relative permittivity of mineral oil, experiments were conducted to determine the speed of the electromagnetic waves emitted by the PD source and propagating in oil. This was found to be $2x10^8$ m/s (i.e. two thirds the speed of light) [10].

5.2 SIGNALS WAVEFORM PATTERNS

The electromagnetic waves generated by the PD source inside the transformer tank will propagate toward all directions. During the propagation, the signals may encounter internal barriers or the transformer tank and thus reflection and/or refraction of the PD signals may occur. This can distort the signal waveforms, resulted in different waveform patterns and can lead to error in the TDOA values, especially for the cross-correlation method.

The PD signal patterns are also very much affected by the sensors location. Different locations may produce different patterns. This might be because the initial wave-front of the field radiated by the PD source is not uniform in all directions and the PD signals may be attenuated along its path. Also different sensor positions may see different reflection patterns. Thus the first part of the signal which arrives via a direct path may be quite similar, but the superposition of subsequent multiple reflections will distort the remaining part of the waveforms. Figure 3 shows the PD signals captured by two sensors that were placed at different positions. The signal wave-fronts show similar pattern but after a short duration the waveforms have different shape and magnitude.

Another factor affecting the PD waveform pattern is the sensor type in use in detecting the PD signals. In the experiment, four monopole sensors were employed. Previous work by the authors [19] found that the monopole sensor has lower sensitivity and bandwidth as compared to disk-type sensors. However, it has faster signal response [10, 12] and less oscillation. Consequently, the monopole sensor type was chosen to detect the PD signals in this work. Figure 4 shows the step-pulse response of the monopole sensor and the log-spiral planar type sensor.

5.3 DENOISING THE PD SIGNALS

In practical substation environment, noise or interference mainly consists of continuous sinusoidal-carrier signals (radio frequency) from telecommunication systems, transients caused by thyristor operation or network switching, and thermal noise associated with the detection system [3, 4]. By virtue of its construction, the transformer tank acts as an RF shield against the radiated noise to a certain extent but conductive noise can still propagate into the tank and affect the measurement. Note that here the experiments were conducted in the laboratory where the noise level encountered is much less compared to the substation environment. Figure 5 shows the background noise level recorded by spectrum analyser (without presence of PD activity inside the transformer). Evidence of interference from communication signals can be seen at around 200 to 500 MHz for digital radio and TV, and at around 850 and 900 MHz for mobile communication systems [20]. It should be noted that a broadband measurement system is susceptible to such interference. If the frequency locations of the interference are known then a narrow-band measurement system can be used to tune away from the affected areas and thus avoid the need for extensive denoising.

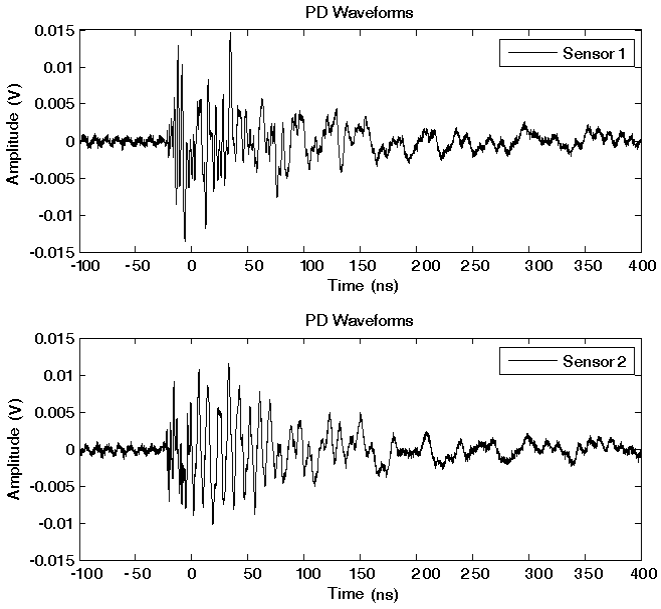

Figure 3. Time domain of the PD signals captured simultaneously by two sensors at different positions.

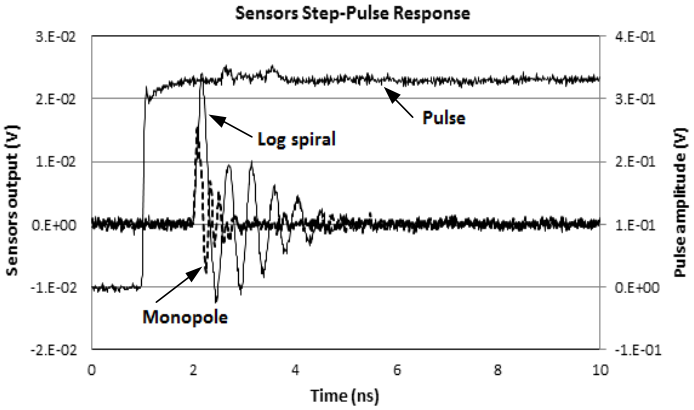

Figure 4. Step-pulse responses of monopole and log-spiral sensors.

In this paper, to denoise the PD signals, multivariate denoising tool is applied [6]. Multivariate wavelet denoising deals with regression models of the form:

$$X(t_i) = f(t_i) + \varepsilon(t_i) \tag{4}$$

where:

$i \in [1, \cdots, N]$ and N is number of data points

$X(t_i)$ = observed signal

$\varepsilon(t_i)$ = centered Gaussian white noise of unknown variance

$f(t_i)$ = unknown function to be recovered

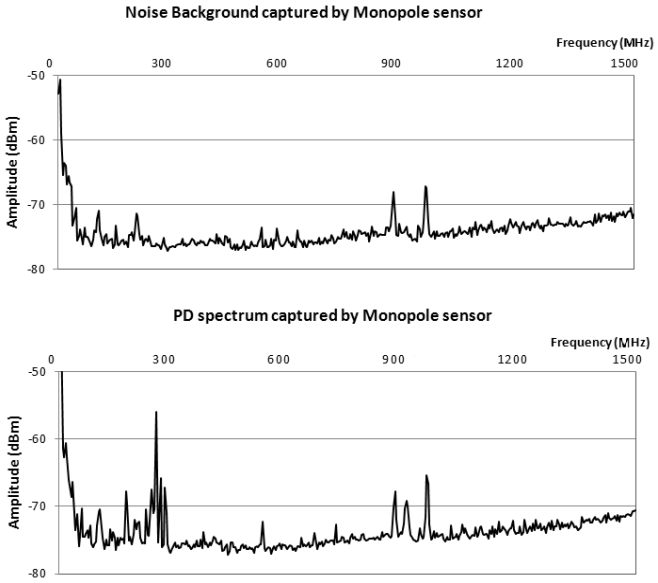

Figure 5. Noise background and PD spectrum captured by monopole sensor installed inside transformer tank.

The multivariate denoising procedure is carried out in two stages. The original signal, for example Figure 6a, is first decomposed using the wavelet transform, and then denoised by applying multivariate thresholding. The result of the first step is shown in Figure 6b. To improve the denoising, a further step is performed using principal component analysis (PCA). The result is shown in Figure 6c. Compared to Figure 6b, there is some improvement although very marginal. Details of PD signal denoising process can be found in [10].

6 TIME DIFFERENCE OF ARRIVAL CALCULATION

The location of the PD source in the transformer tank can be estimated by utilizing the arrival time difference between signals (TDOA) captured by the sensor array. Three methods to calculate the TDOA are described in this section and their performances compared in the following section.

6.1 FIRST PEAK METHOD

Assuming the signals in the transformer tank propagate in same manner toward all directions, the sensors will capture the same PD pulse and produce similar waveforms. The arrival time difference between signals then can be determined from the first peaks of the waveforms recorded by different sensors. The first peak is defined as the first time instant when the signal amplitude exceeds a certain level [7, 10]. Such a minimum threshold is necessary to counter the presence of noise in the signals which is unavoidable even after the application of denoising. Previous work using this method relied on human intervention (visual inspection) to determine the first peaks. This is not convenient, particularly when a large set of waveforms is involved. In this work, an algorithm is introduced so that the first peak points can be automatically calculated with a program written in Matlab codes. It scans through the data array consecutively and compares each point in the waveforms to a value before. If the value decreases, the last higher value is taken as a peak. The first peak is defined as the first occurrence of a peak whose value exceeds a specific threshold.

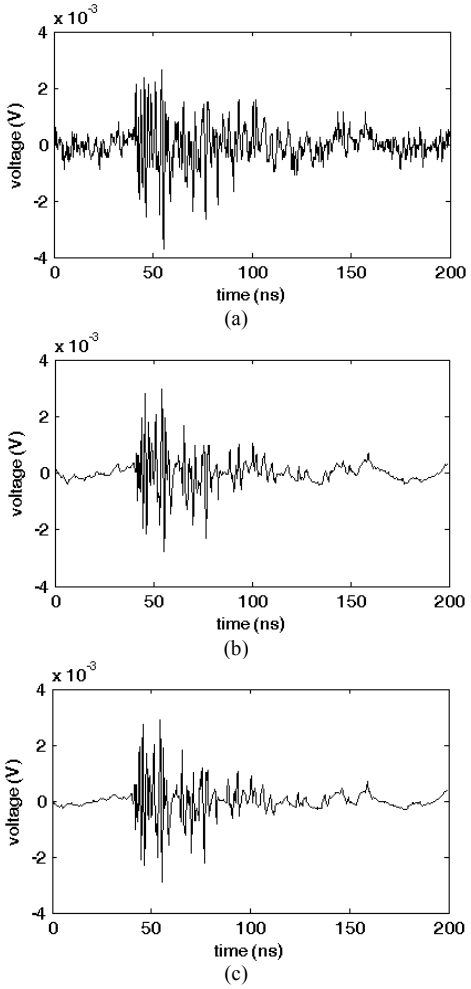

Figure 6. (a) original signal, (b) denosing using multivariate thresholding, and (c) result after retaining PCA component [10].

The procedure to determine the TDOA between the first peaks of PD signals captured by 2 sensors is as follows:

1. Denoise the original signal by applying multivariate denoising tool. The denoising process is done to the PD signals captured at the same time frame by the sensors.
2. Process both the original (undenoised) and denoised signals to make the waveforms unipolar, achieved by taking absolute value of each point of the waveform.
3. Normalize the signals so all the waveforms have similar magnitude.
4. Choose the same threshold setting, for example 25% of the signals magnitude.
5. Pick the first peak point above the threshold value by applying the peak point detector. This point is then used to determine the arrival time. Figure 7 shows an example of result from applying steps 1 to 5.

6. Calculate the time difference between the two first peaks of the PD signals.

From Figure 7 and applying a signal threshold of 25%, the TOA for sensor 1 is 84.950 ns and that for sensor 4 is 84.425 ns. Thus the TDOA between these particular waveforms is 0.525 ns.

6.2 CROSS-CORRELATION METHOD

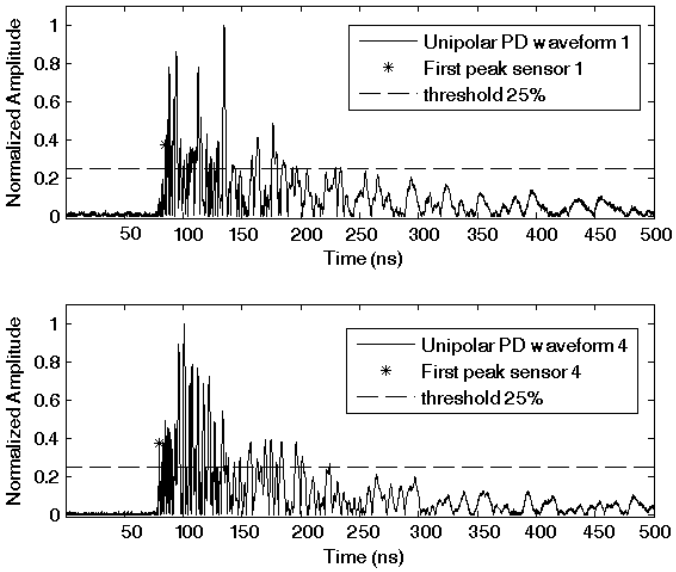

Figure 7. Peaks of normalized unipolar denoised PD waveforms.

The TDOA between two sensor signals also can be determined by using cross-correlation between the signals. Cross-correlation measures the similarity between two waveforms as a function of a time lag applied to one of them. One waveform is considered in stationary position and other is shifted toward the stationary one. The similarity between these two waveforms is then calculated. The TDOA is determined as the location where the cross-correlation curve reaches its peak. For perfectly uncorrelated such as random functions, the cross-correlation value is zero.

The cross correlation $f(t)$ of two continuous functions $g(t)$ and $h(t)$ is defined as:

$$f(t) \equiv \int_{-\infty}^{+\infty} \overline{g}(\tau) h(t+\tau)\, d\tau \tag{5}$$

where $\overline{g}$ denotes the complex conjugate of g. If the functions are discrete, the cross correlation is similarly defined as:

$$f(n) \equiv \sum_{-\infty}^{+\infty} \overline{g}(m) h(n+m) \tag{6}$$

Furthermore, if these discrete functions are time series of finite duration then [21]:

$$f(n) \equiv \frac{1}{N} \sum_{m=0}^{N-|n|-1} g(m) h(n+m) \tag{7}$$

where N is the number of data points.

Figure 8 shows an example of the cross-correlation between the signal captured by the reference sensor 4 and that from the other three sensors. The TDOA is determined from the offset (in terms of data point number) between the peaks. The reference is the peak of the auto-correlation. Each data point offset corresponds to 25 ps. In this particular case, the offsets are 47, 146, -24 data points for sensors 1, 2, 3 respectively which translate to TDOAs of 1.175 ns, 3.650 ns and -0.600 ns. It should be noted that the presence of the core and winding assembly in the tank will exacerbate the difference between the transmission paths to the sensors and thus the cross-correlation would be much more diminished.

6.3 CUMULATIVE ENERGY METHOD

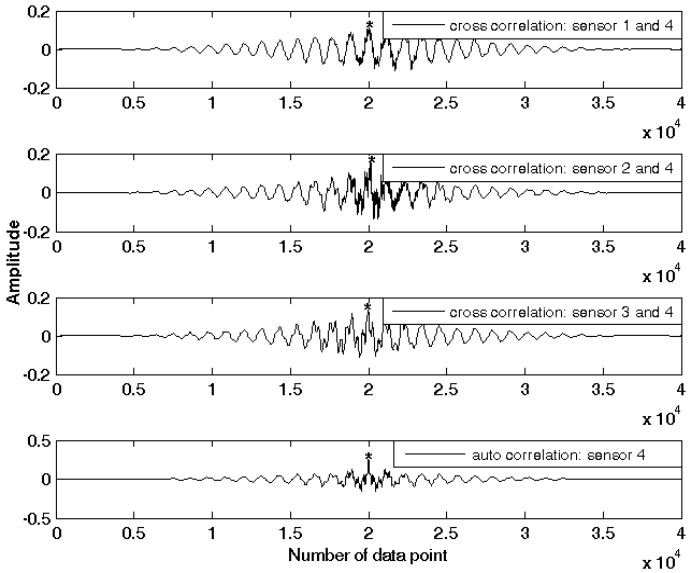

Figure 8. Cross-correlation of the waveforms between sensor k (k = 1,2,3) and reference sensor 4. The peaks are marked with *. PD source is at location 5.

Time difference determination by applying the cross-correlation method is made on the assumption that the PD waveforms have similar pattern. In cases where the patterns are too dissimilar, the cross-correlation method might be not applicable. An alternative solution is to apply a similar concept to calculate the TDOA from the cumulative energy curves of the PD waveforms.

When the sensors are installed in 'quite far' from each other, the PD waveforms received tend to have different patterns [10]. However, the energy of the PD signals can be assumed to be dependent on the distance from the PD source [22]. By converting the PD amplitude to the cumulative energy [7, 10], a similar trend is expected for the increase in the cumulative energy with time. Therefore, the time difference can be determined from these cumulative energy curves.

The PD waveforms are usually captured using a high-bandwidth oscilloscope or digitizer and the results are recorded in terms of voltage magnitude versus time. Given a fixed measuring impedance R and since $Energy = \int \left(V^2/R\right) dt$, the cumulative energy can be determined from the square of

the voltage curve. Thus the cumulative energy up to time t_k and normalized to a resistance of 1 ohm can be expressed as:

$$U(t_k) = \sum_{i=1}^{k} \left(V(t_i)\right)^2 \quad (8)$$

where $V(t_i)$ is the sampled input signal at time t_i. If N is the total number of data samples in each voltage curve (20000) then $U(t_N)$ corresponds to the total energy of the signal.

Figure 9 shows a typical example. The time differences between signals are acquired from the cumulative energy curves by exploiting a unique point in the curves. The most significant point that can be used to determine the arrival time of the signal and thus to determine the time differences between sensors is the 'knee point'. This is defined as the point where a 'sudden' increase in the cumulative energy occurs [7, 9, 22]. No mathematical definition was provided for quantifying this condition. Thus, the interpretation of the knee point by different observers may result in different times of the arrival of the signals. Since this not only causes ambiguous result but also is time-consuming and tedious, the knee point method was not further investigated in this paper.

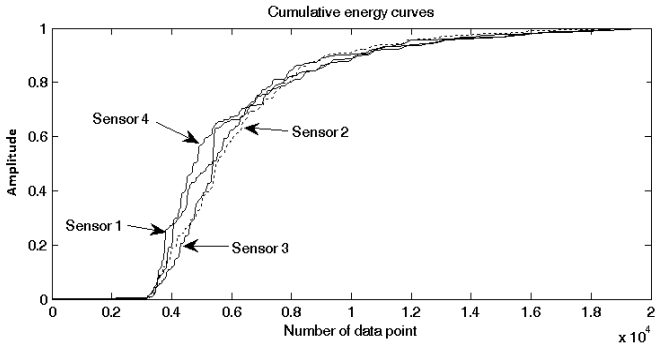

Figure 9. Normalized cumulative energy curves of sensor voltage waveforms (PD at position 1).

The other method is by applying a similarity function between the cumulative energy curves. The time difference is calculated from this mathematical operation. Here, one curve is time-shifted toward the other by some amount and then the extent of similarity (overlapping) between these two curves is determined from:

$$S(t_k) = \sum_{i=1}^{N-k} \left| U_1(t_i) - U_2(t_{i+k}) \right| \quad (9)$$

where U_1 and U_2 are the two cumulative energy curves. k denotes the amount of shifting, each increment corresponds to a time step of 25ps. U_1 and U_2 are also interchanged to produce shifting in the opposite direction. The process is iterative and the solution is found when the similarity value reaches the minimum.

During its propagation, the PD signal will be attenuated and reflected by the transformer tank and other physical components inside the tank. The sensors capture not only the original PD signal but also the subsequent reflections so the signals captured by sensors at different positions have similar waveform patterns only during the initial period when the reflections are yet to arrive. The same effect applies to the cumulative energy of the PD signals. Thus if the complete waveform data are used to determine the time difference the result might give higher error [10, 11]. To reduce the error, [11] suggested using only part of the PD waveform, i.e. the front part of the PD waveform, to evaluate the cumulative energy. This was done by setting a time window with specific length. However, manually determining the length of the windows is very subjective. Such a task is imprecise and strongly influenced by how the observer interprets the waveforms. In order to avoid this ambiguity, one can assign a fixed percentage of the data for use in the cumulative energy calculation [10].

7 PD LOCALIZATION

The PD location can be calculated using equations (2) and (3). The TDOAs which are acquired using the three methods are used as r_{i4} in equation 3. The calculated PD coordinates for each method are shown in each section. The average error results for all methods and for both the original (noisy) and denoised signals are shown in Table 7.

7.1 FIRST PEAK METHOD

The calculated coordinates using the first peak method are shown in Table 3. All location results show the PD source inside the transformer tank. The coordinates acquired by both original and denoised signals show quite similar values.

Table 3. The coordinates of the PD location of first peak method.

PD loc.	Original x,y,z (cm)	Denoised x,y,z (cm)
1	-1.84, 0.04, 37.99	-2.00, 0.52, 44.28
2	-2.21, 0.58, 44.21	-2.18, 0.81, 43.87
3	-2.26, -0.24, 46.74	-1.92, 0.56, 37.24
4	-2.45, -1.12, 57.52	-2.22, -0.82, 50.64
5	-1.51, 0.98, 33.36	-1.66, 1.09, 37.79
6	-1.85, 0.55, 45.29	-1.32, 1.71, 30.74
7	-1.88, -0.5, 46.05	-1.49, -0.25, 37.95
8	-1.59, 0.59, 40.97	-1.32, 0.69, 37.52
9	-2.21, 1.03, 51.96	-1.96, 0.71, 36.57
10	-0.87, -0.34, 41.9	-0.75, -0.96, 52.54
11	-1.79, 1.56, 61.11	-3.89, -4.79, 45.3
12	-1.41, 1.29, 47.87	-1.24, 0.99, 42.07

From Table 7, it can be seen that the denoising process improves the localization results. Out of 12 PD locations, 10 locations resulted in improvement of the PD location accuracy and only 2 show the opposite result. The highest error when using the original waveforms is 27.99 cm and this reduces to 20.42 cm after the waveforms are denoised.

7.2 CROSS-CORRELATION METHOD

Table 4 shows the coordinates of PD localization using the cross-correlation method. Some cases show the coordinates outside the transformer tank and hence produce large errors as seen in Table 7. The cross-correlation was carried out by using the full recorded waveform with a time duration of 500 ns. Note that this corresponds to EM waves propagation in oil over a distance up to 100 m whereas the largest dimension of

the transformer tank (width) used in this work is just 1 m. Thus the recorded signal over such a long duration will certainly capture multiple reflections of the original PD pulse and may also include other PD pulses as well. This can cause error on the TDOA results and yield false PD localization.

Table 4. The coordinates of the PD location calculated using cross-correlation method. (full length of waveform).

PD loc.	Original x,y,z (cm)	Denoised x,y,z (cm)
1	-0.65, -4.56, 14.42	-0.51, -4.65, 15.38
2	0.58, -6.42, -13.44	2.21, -8.73, -48.32
3	4.69, -10.62, -76.43	3.39, -9.24, -55.51
4	-1.49, -4.00, 22.83	-0.63, -4.97, 7.75
5	0.20, -5.85, -5.57	0.43, -6.17, -10.59
6	0.12, -5.72, -3.56	0.12, -5.73, -3.72
7	-0.09, -5.46, 0.55	-0.16, -5.55, 2.06
8	0.06, -5.54, -2.08	-0.10, -5.46, 1.47
9	-0.09, -5.40, 1.47	-0.01, -5.50, -0.11
10	-0.79, -3.09, 36.87	-1.04, -2.99, 38.42
11	-0.12, -5.37, 2.08	-0.16, -5.27, 3.58
12	-0.08, -5.33, 2.25	-0.08, -5.33, 2.18

The cross-correlation method can be improved by post-processing the data and using only the initial data record with length comparable to the transformer dimension. For this particular experiment setup, applying a time window of 5 ns after triggering would be a reasonable choice to filter out the reflections from the recorded data. The new PD coordinates resulted by applying this approach are shown in Table 5. It can be seen that only one case (at location 3) shows a coordinate located outside the transformer tank but this error was much reduced after denoising. The resultant accuracy is much better than using the full length of waveforms.

Table 5. The coordinates of the PD location calculated using cross-correlation method. (5 ns of waveform).

PD loc.	Original x,y,z (cm)	Denoised x,y,z (cm)
1	-3.76, 0.41, 44.63	-1.05, -1.03, 51.02
2	-3.58, 6.74, 68.85	-0.28, -4.44, 1.89
3	-4.80, -0.33, -6.79	-5.60, -2.92, 47.46
4	-3.78, 8.05, 62.82	-1.24, -3.28, 25.93
5	-3.56, 4.58, 64.46	-1.08, -3.10, 28.6
6	-3.35, 2.32, 68.54	-2.14, -2.56, 37.01
7	-4.93, 4.87, 0.13	-7.06, -1.18, 68.86
8	-4.35, -2.60, 8.66	-4.61, -3.50, 24.4
9	-4.52, -3.08, 0.52	-4.39, -2.30, 2.11
10	-5.01, 6.12, 0.48	0.53, -2.29, 42.09
11	-4.64, 5.93, 16.63	0.43, -2.13, 44.27
12	-3.88, -3.15, 29.96	-4.40, -4.82, 18.5

Similar to the first peak results, the results for the cross-correlation method show improvement after the waveforms are denoised in 8 out of 12 locations tested. The worst-case error produced from using original waveform is 44.38 cm (PD location 3). After the waveform is denoised, the error is down to 11.82 cm.

7.3 CUMULATIVE ENERGY METHOD

The calculated coordinates using the cumulative energy method are shown in Table 6. Out of 12 different PD locations, only one shows a coordinate outside the tank. From Table 7, the denoising process appears to produce random results with only 5 out of 12 PD locations produced better accuracy after denoising.

Table 6. The coordinates of the PD location calculated using cumulative energy function

PD loc.	Original x,y,z (cm)	Denoised x,y,z (cm)
1	-0.91, -2.91, 43.4	-2.25, -3.69, 44.06
2	-1.18, -2.98, 51.43	6.27, -22.48, 0.38
3	-1.61, -2.47, 58.19	6.15, -12.84, 36.86
4	-3.27, -1.49, 62.15	-3.3, -2.3, 45.82
5	-3.19, 0.31, 62.48	-2.85, -0.76, 46.37
6	-2.1, 1.18, 55.57	-14.85, -1.33, -9.25
7	-3.59, -2.49, 47.89	-4.59, 32.71, 59.45
8	-2.57, -2.29, 48.83	-3.05, 2.61, 42.96
9	-3.31, -1.5, 59.74	-10.7, 14.46, 69.29
10	-4.26, -2.47, 48.5	-3.52, -2.49, 47.11
11	-2.54, -0.15, 47.62	-2.92, 22.88, 56.27
12	-3.3, 0.94, 53.3	-11.93, 7.83, 67.82

The above result indicates that for the cumulative energy method, the denoising process shows no positive effect on the PD localization accuracy while the denoising process itself increases the computation burden. With or without the denoising process, this method consumes more computation time as compared to the other two methods. Improvement may be achieved [11] by windowing the captured record so only those data points associated with the PD waveform are included in the calculation, i.e. discard further data points when the signal has completely decayed. This would significantly reduce the computation of equations (8) and (9) which is dependent on the number of data points involved. However, to carry out such a windowing requires either human involvement or additional computation.

7.4 COMPARISON BETWEEN METHODS

The comparison of the localization using the three methods is summarized in Table 7. The first peak method has the highest accuracy. Overall average errors for original and denoised waveforms are 16.65 cm and 14.33 cm respectively.

Table 7. Average errors of the PD localization: (a) original, (b) denoised.

PD Loc.	First Peak (cm)		Cross-correlation (cm)		Cumulative energy (cm)	
	(a)	(b)	(a)	(b)	(a)	(b)
1	16.73	17.76	17.19	22.84	20.71	20.96
2	12.20	11.94	32.75	37.9	19.19	48.93
3	13.61	10.17	44.38	11.82	23.23	19.29
4	25.50	20.15	26.5	20.6	29.54	18.54
5	5.62	4.21	27.47	11.82	25.91	11.00
6	9.53	8.64	32.16	1.67	19.3	47.82
7	19.60	17.01	40.01	38.04	22.73	30.49
8	9.63	8.51	31.12	18.54	16.32	11.1
9	18.10	9.80	39.01	40.55	24.82	41.23
10	20.62	25.67	42.10	21.37	26.49	25.48
11	27.99	20.42	26.31	15.41	18.72	30.23
12	18.37	15.39	17.46	24.72	23.13	41.07
Average	16.65	14.33	31.37	22.11	22.51	28.84

For the cross-correlation method, the overall average error is 31.37 cm for original signals and reduces to 22.11 cm after the signals were denoised. Compared to the first peak method, the cross-correlation method yields less accurate results. This indicates that sensors at different positions will not receive

exactly identical waveforms even after further processing has been applied to remove possible corruption at the tail end of the signals.

For the cumulative energy method, the average errors by the denoised cumulative energy curve method are mostly higher than the corresponding results from the cross-correlation method. The overall average errors are 22.51 cm and 28.84 cm for the original and denoised PD signals respectively.

A graphical approach to present the results is by plotting circles (on x-y plane) around the true PD locations. Their radii correspond to location errors obtained from various methods

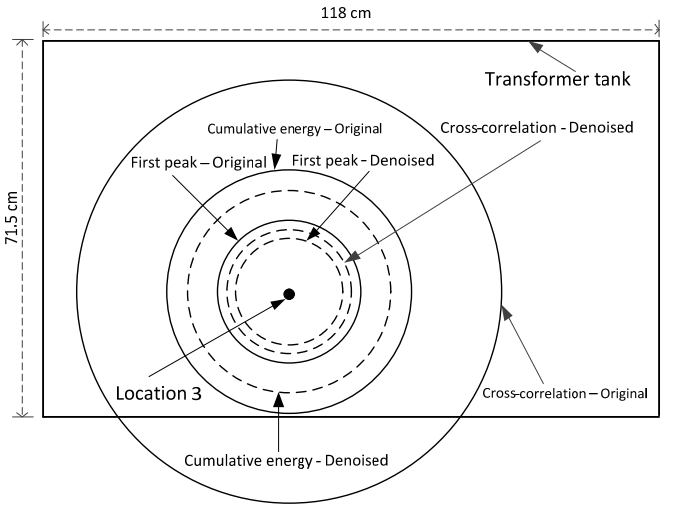

(a)

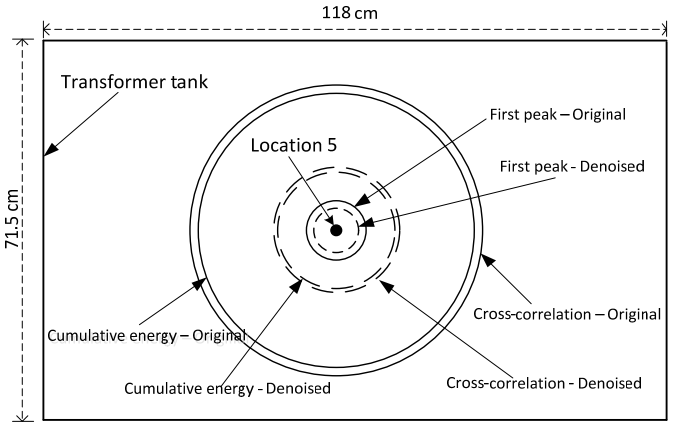

(b)

Figure 10. PD localization error plots: (a) PD location 3, (b) PD location 5.

(Table 7). Results for two different PD locations (3 and 5) are shown in Figure 10.

Compared to PD location based on the acoustic/ultrasonic pressure wave detection which deals with low-frequency signals (~100 kHz) with very slow propagation velocity (~1200 m/s), UHF signals give a much sharper transition which is advantageous for accurate measurement of signal arrival time. On the other hand, the very fast propagation velocity of UHF signals combined with the dimensional effect of the small experimental tank used here presents a challenge. By and large, location error results from Table 7 appear to indicate ~20 cm as representative. As the propagation velocity of EM waves in oil is 20 cm/ns, an error of 20 cm in distance corresponds to 1 ns in signal propagation time. Considering the sampling rate is quite adequate (25 ps in between samples), it is likely that there are other factors contributing to the uncertainty in the timing of signals and thus required further investigations.

8 CONCLUSION

This paper discussed the application of three methods to determine the time difference of arrival (TDOA) between PD signals simultaneously captured through an array of four UHF sensors. Each set of such signals enables TDOA calculation of three signals with respect to the remaining reference signal. From this information, an explicit solution for the PD location can be found using an efficient software realization of the maximum-likelihood estimator.

Among the three methods of TDOA determinations, the method based on finding the signal first peak was found to give the best accuracy, followed by the cross-correlation, and lastly the cumulative energy. Typical (overall average) errors are 14.33, 22.11, and 28.84 cm respectively. These results were achieved with additional denoising. Although denoising produces consistent accuracy improvement when applied to the first peak method, its effect is reduced or even adverse for the other two methods. Among all the different test configurations, the best result was achieved with the first peak combined with denoising, resulting in a location error of 4.21 cm. Considering the small dimension of the transformer tank tested (71.5x118x95 cm), care should be taken in extrapolating the observations here to large transformers where the sensors are much more widely spaced and thus likely to encounter physical barrier blocking their line-of-sight view.

REFERENCES

[1] M. D. Judd, G. P. Cleary, C. J. Bennoch, J. S. Pearson and T. Breckenridge, "Power transformer monitoring using UHF sensors: site trials", IEEE Conf. Electr. Insul. (EIC), Boston, USA, pp. 145-149, 2002.

[2] M. D. Judd, L. Yang and I. B. B. Hunter, "Partial discharge monitoring of power transformers using UHF sensors. Part I: sensors and signal interpretation", IEEE Electr. Insul. Mag., Vol. 21, No. 2, pp. 5-14, 2005.

[3] L. Yang, M. D. Judd and C. J. Bennoch, "Denoising UHF signal for PD detection in transformers based on wavelet technique", IEEE Conf. Electr. Insul. Dielectr. Phenomena (CEIDP), Colorado, USA, pp.166-169, 2004.

[4] M. Florkowski and B. Florkowska, "Wavelet-based partial discharge image denoising", Proc. IET - Generation, Transmission & Distribution, Vol. 1, No. 2, pp. 340-347, 2007.

[5] C. Zhou, D. M.Hepburn, X. Song and M. Michel, "Application of Denoising Techniques to PD measurement Utilising UHF, HFCT, Acoustic Sensors and IEC60270", Int'l. Conf. Electricity Distribution (CIRED), Prague, Czech Republic, pp. 1-4, 2009.

[6] M. Aminghafari, N. Cheze and J. M. Poggi, "Multivariate de-noising using wavelets and principal component analysis", Computational Statistics & Data Analysis, No. 50, pp. 2381-2398, 2006.

[7] P. Kakeeto, M. D. Judd, J. Pearson and D. Templeton, "Experimental investigation of positional accuracy for UHF partial discharge location", IEEE Int'l. Conf. Condition Monitoring and Diagnosis (CMD), Beijing, China, pp. 1070-1073, 2008.

[8] X. Song, C. Zhou and D. M. Hepburn, "An Algorithm for Indentifying the Arrival Time of PD Pulses for PD Source Location", IEEE Conf. Electr. Insul. Dielectr. Phenomena (CEIDP), Québec City, Canada, pp. 379-382, 2008.

[9] Y. Jing-gang; L. Da-jian; L. Junhao; Y. Peng and L. Yan-ming, "Study of time delay of UHF signal arrival in location partial discharge", IEEE Int'l. Conf. on Condition Monitoring and Diagnosis (CMD), Beijing, China, pp. 1088-1092, 2008.

[10] H. H. Sinaga, B. T. Phung, P. L. Ao and T. R. Blackburn, "Partial Discharge Localization in Transformers Using UHF Sensors", IEEE Conf. Electr. Insul. (EIC), Annapolis, USA, pp. 64 – 68, 2011.

[11] Z. Tang; C. Li; X. Cheng; W. Wang; J. Li and J. Li, "Partial discharge location in power transformers using wideband RF detection", IEEE Trans. Dielectr. Electr. Insul, Vol. 13, pp. 1193–1199, 2006.

[12] P. J. G. Orr, A. J. Reid and M. D. Judd, "Sensor response characteristics for UHF location of PD sources", IEEE Int'l. Conf. Condition Monitoring and Diagnosis (CMD), Beijing, China, pp. 1119-1122, 2008.

[13] G. P. Cleary and M. D. Judd, "UHF and current pulse measurements of partial discharge activity in mineral oil", IEE Proc. of Sci. Meas. Technol., Vol. 153, No. 2, pp. 47-54, 2006.

[14] W. H. Foy, "Position-location solutions by Taylor-series estimation", IEEE Trans. Aerospace Electronic System, Vol. 12, pp. 187-194, 1976.

[15] D. J. Tonieri, "Statistical theory of passive location systems", IEEE Trans. Aerospace Electronic System, Vol. 20, pp. 183-198, 1984.

[16] B. X. Du, Y. H. Lu, G. Z. Weil and Y. Tian, "PD Localization Based on Fuzzy Theory using AE Detection Techniques", IEEE Conf. Electr. Insul. Dielectr. Phenomena (CEIDP), Nashville, USA, pp. 449-453, 2005.

[17] H. C. Schau and A. Z. Robinson, "Passive source localization employing intersecting spherical surfaces from time-of-arrival differences", IEEE Trans. Acoust., Speech, Signal Processing, Vol. 35, pp. 1223-1225, 1987.

[18] Y. T. Chan and K. C. Ho, "Simple and Efficient Estimator for Hyperbolic Location", IEEE Trans. Signal Processing, Vol. 42, pp. 1905-1915, 1994.

[19] H. H. Sinaga, B. T. Phung, T. R. Blackburn, "Design of ultra high frequency sensors for detection of partial discharges", Int'l. Symp. on High Voltage Engineering (ISH), Cape Town, South Africa, pp. 892-896, 2009.

[20] H. H. Sinaga, B. T. Phung, P. L. Ao and T. R. Blackburn, "Partial Discharge Measurement for Transformer Insulation Using Wide and Narrow Band Methods in Ultra High Frequency Range", Australasian Universities Power Engineering Conf. (AUPEC), Adelaide, Australia, paper PP027, pp.1-5, 2009.

[21] S. J. Orfanidis, *Optimum Signal Processing. An Introduction*, 2nd ed., Prentice-Hall, Englewood Cliffs, NJ, 2007.

[22] S. Meijer, R. A. Jongen, E. Gulski and J. Smit, "Location of Insulation Defects in Power Transformer Based on Energy Attenuation Analysis", IEEE Int'l. Symp. on Electrical Insulating Materials (ISEIM), Kitakyushu, Japan, pp. 698-702, 2005.

Herman Halomoan Sinaga (S'2010) received the B.S. degree in electrical engineering from the University of North Sumatera, Indonesia, in 1997 and the M.S. degree in electrical power engineering from the Gadjah Mada University, Indonesia, in 2001. He is currently studying toward the Ph.D. degree at the University of New South Wales, Australia. Since 1999, he has been a Faculty Member with the Department of Electrical Engineering, Lampung University, Indonesia. His areas of research interest include electrical insulation and condition monitoring of power system equipment.

B. T. (Toan) Phung is currently a Senior Lecturer at the University of New South Wales, School of Electrical Engineering and Telecommunications. His Ph.D. degree work was on computer-based partial discharge detection and characterization. His main research interests are in electrical insulation materials, high-voltage engineering and on-line condition monitoring of power system equipment. He is an IEEE senior member and a member of the CIGRÉ Australian Panel D1.

T. R. (Trevor) Blackburn is currently a Visiting Associate Professor at the University of New South Wales, School of Electrical Engineering and Telecommunications. He received the Ph.D. degree in electrical engineering from Flinders University, Australia. His principal research and teaching interests are in power equipment condition monitoring and gas discharges, particularly in the partial discharge monitoring and lightning applications. He is a member of a number of working groups, concerned with condition monitoring, of Study Committee SC D1 of CIGRÉ. He has organized and lectured a number of short courses on Condition Monitoring and Partial Discharges and Electrical Safety.